

# IMPROVED VEHICLE PARAMETER ESTIMATION USING SENSOR FUSION BY KALMAN FILTERING

*Erik Steinmetz*<sup>1</sup>, *Ragne Emardson*<sup>2</sup>, *Per Jarlemark*<sup>3</sup>

<sup>1</sup> SP Technical Research Institute of Sweden, Borås, Sweden, [estein@etek.chalmers.se](mailto:estein@etek.chalmers.se)

<sup>2</sup> SP Technical Research Institute of Sweden, Borås, Sweden, [ragne.emardson@sp.se](mailto:ragne.emardson@sp.se)

<sup>3</sup> SP Technical Research Institute of Sweden, Borås, Sweden, [per.jarlemark@sp.se](mailto:per.jarlemark@sp.se)

**Abstract** – Within several applications concerning the improvement of vehicle safety, accurate systems for determination of position, velocity and acceleration are useful. We present a system for accurate determination of these parameters using a sensor fusion technique. The main focus is on how GPS carrier phase data and accelerometer data are modeled and integrated in a Kalman filter that provides both estimates and accompanying uncertainties.

**Keywords:** Sensor fusion, Kalman filter, Global positioning system (GPS)

## 1. INTRODUCTION

Accurate information about position, velocity and acceleration is useful for several applications with the aim of improving vehicle safety. In for example advanced outdoor crash tests, studies of wind loads on cars and driver behaviour knowledge about position, velocity and acceleration at high sampling rates are important. We present a system for accurate determination of position, velocity and acceleration of a vehicle, by using a sensor fusion technique for combining GPS carrier phase technology with accelerometers to achieve an increased time resolution.

The main focus in the paper is on how the GPS carrier phase data and accelerometer data are integrated in a multi rate Kalman filter and how the system is modeled as well as how process parameters are determined.

## 2. STATE-OF-THE-ART GPS/INS INTEGRATION

Kalman filter algorithms are widely used in the field of navigation to integrate different navigation sensors such as GPS and Inertial Navigation Systems (INS) in order to exceed the performance of the individual sensors.

Smyth et al. [1] shows by simulations the advantages of combining information from displacement sensors and accelerometers in dynamic system monitoring. The method provides improved estimates of velocity and displacement,

avoiding low frequency noise amplification from the accelerometers and high frequency noise amplification from the displacement measurements. Smyth et al. also brings up the fact that higher sampling rates are available with accelerometers and that this also can be used to increase the limited time resolution in GPS (State of the art GPS samples with a rate of 20 Hz). The maximum sampling rate of the measured acceleration was set to 1000 Hz in their simulations.

Most integrated navigation systems are today, as in [1], loosely coupled [2], which means that displacement data (in most cases GPS position estimates) are integrated with INS data in the navigation filter. However, tightly coupled systems where raw GPS data, in the form of pseudoranges/delta-ranges, instead of positions, are directly integrated with INS data are often superior [2]. Such an algorithm is demonstrated and tested in [2] together with a method where time differenced GPS carrier phase measurements are used to improve the accuracy of the velocity estimates.

Relative GPS carrier phase measurements can be used to reach centimeter accuracy in the estimated positions. Gao et al. [3, 4] presents a centimeter level vehicular positioning system, using GPS/INS G-sensors/yaw rate sensors and wheel speed sensors, with focus on maintaining accuracy during GPS outages. The system uses GPS carrier phase measurements with resolved integer ambiguities and provides position, velocity and attitude at an update rate of 20 Hz. Also Kim et al. [5] presents simulations from a complete GPS/INS integration algorithm with GPS carrier phase measurements.

Integer ambiguity determination and cycle slip detection can be improved by using INS information. Kim et al. [5] suggests an INS aided integer ambiguity resolution algorithm. Petovello et al. [6] also shows the advantages of using INS information. They present an ultra-tight GPS/INS navigation strategy for centimeter-level GPS carrier phase positioning in weak signal environments, by using a software based receiver with INS aided tracking loops. This method provides a sensitivity improvement in terms of position accuracy, and they suggest that with this technique

the RTK capability could be expanded in weak signal applications, with difficulties to track the carrier phase.

This paper presents high precision (centimeter level) estimation of position, velocity and acceleration for a moving vehicle with an update rate of 1000 Hz. This is achieved by combining GPS and accelerometer data in a tightly coupled multi-rate Kalman filter algorithm. Relative GPS carrier phase measurements are used to achieve the obtained precision in the position, velocity and acceleration.

### 3. MEASUREMENTS

The developed system consists of accelerometers and GPS receivers. Two accelerometers are mounted in the vehicle perpendicular to each other so that one accelerometer measures the acceleration in the driving direction and the other one measures the acceleration sideways. Both accelerometers measure the acceleration with a sampling rate of 1 kHz. Due to the design of the accelerometers frequency components below 0.2 Hz are not captured. The accelerometer measurements are then transformed to the GPS coordinate system by multiplying them with a transformation matrix  $T$ , where  $\theta$  is the angle between the two coordinate systems. A simplification is here made of the coordinate systems and the accelerometer data is only projected into the horizontal components of the GPS coordinate system.

$$T = \begin{pmatrix} \cos \theta & -\sin \theta \\ \sin \theta & \cos \theta \end{pmatrix} \quad (1)$$

$$\begin{pmatrix} X_{GPS} \\ Y_{GPS} \end{pmatrix} = T \begin{pmatrix} X_A \\ Y_A \end{pmatrix}$$

The GPS equipment consists of a reference antenna and receiver positioned at a known location and an antenna and a receiver mounted on the vehicle, referred to as the rover. Both GPS receivers measure the received signal phase at the respective antenna at two different frequencies,  $f_1$  and  $f_2$ . The observed phase is sampled at a frequency of 20 Hz.

The phase measurements from the rover and the reference receiver can be described by (2) and (3), where  $\varphi$  is the measured phase in fraction of cycles,  $\rho$  is the geometrical distance between the receiver and the satellite,  $N$  is the integer number of cycles referred to as the ambiguity parameter. The  $\delta t$  represents the combined satellite and receiver clock error,  $l_o$  is the error in the reported satellite position,  $l_i$  is the signal delay in the lower part of the atmosphere referred to as the troposphere,  $l_i$  is the signal delay in the ionosphere part of the atmosphere, and  $\varepsilon$  is measurement error.  $\lambda$  is the signal wavelength and  $f$  is the signal frequency [7].

$$\varphi_A = \frac{1}{\lambda} \rho_A + N_A + f \delta t_A + l_o + l_i + l_i + \varepsilon \quad (2)$$

$$\varphi_B = \frac{1}{\lambda} \rho_B + N_B + f \delta t_B + l_o + l_i + l_i + \varepsilon \quad (3)$$

By multiplying (2) and (3) with the signal wavelength and subtracting them, we obtain a phase difference measurement:

$$\lambda \Delta \varphi = \Delta \rho + N + c \delta t_D + \Delta l_i + \varepsilon_D \quad (4)$$

In (4), we have assumed that the orbital errors and the ionospheric delay are approximately identical for the two receivers, because the separation is relatively small, and thus cancel each other. The contribution from the troposphere, however, depends on the height difference between the rover and the reference station as the signals at the two antennas experience different amounts of troposphere. The main part of the tropospheric delay that remains can be approximated using height difference information as

$$\Delta l_i = \Delta z \times \chi_0 \times m \quad (5)$$

where  $\Delta z$  is the height difference between the rover and the reference. The parameter  $\chi_0$  is the refractivity coefficient at the surface of the earth [7], and  $m$  is a mapping function used to relate observations in the zenith direction to the direction of the satellite. To achieve the necessary information about the height difference  $\Delta z$  a preliminary estimation of the reference and rover positions are performed using the less precise code observables.

Start values for the integer parameter,  $N$ , in (4) are found from evaluating candidates and choosing one set of integer values that optimizes the match between the models and the measurements. We use the code data to find *a priori* values of  $N$  in this evaluation. The integer values are expected to remain constant in time. There are, however, instants when a receiver temporarily loses the continuous tracking of a certain satellite signal while later resume it. Under such circumstances, the correct value for  $N$  after the break differs an integer number from the previously chosen value for this satellite. In order to detect these cycle slips, the phase observables  $L1$  and  $L2$  at the two frequencies,  $f_1$  and  $f_2$  are compared at two adjacent points in time. The change measured in units of length is expected to be approximately equal at the two frequencies. We form the test

$$\begin{aligned} & (\lambda_{L1} \Delta \varphi_{L1}(t-1) - \lambda_{L2} \Delta \varphi_{L2}(t-1)) - \\ & (\lambda_{L1} \Delta \varphi_{L1}(t) - \lambda_{L2} \Delta \varphi_{L2}(t)) \geq \Psi \end{aligned} \quad (6)$$

where  $\lambda$  is the wavelength for signals at the two different frequencies and  $\varphi$  is the corresponding phase difference in (4), and  $\Psi$  is the test limit. We use a value of 3 mm for  $\Psi$ . This is, with some margin for noise, enough to detect the difficult cycle slip combination of 9 cycles on  $L1$  and 7

cycles on  $L2$ . If the requirement in (6) is fulfilled for a satellite, this satellite is temporarily excluded from the calculations, and a solution is formed from the remaining satellites. We use this solution to determine an  $N$  value for the excluded satellite.

By subtracting the derived  $\Delta I_t$  and  $N$  from the measures in (4) we obtain a set of corrected phase difference measurements that are used in the estimation procedure.

#### 4. SENSOR FUSION

We estimate the discrete states of the sought parameters, position, velocity, and acceleration using a Kalman filter [8]. The measurement model of the filter is the assumed linear relationship between the input quantity, i.e., the measurements,  $z$ , and the output quantity,  $x$ , that we want to estimate. This relationship is described by the observations matrix,  $H$ , containing the partial derivatives

$$z = Hx + v \quad (7)$$

where  $v$  is the measurement noise. The input quantity,  $z$ , contains the corrected phase difference measurements from the two GPS receivers and the acceleration measurements in two directions from the accelerometers. The output quantity,  $x$ , contains the variables

$$x = \{r_e, r_n, r_v, \dot{r}_e, \dot{r}_n, \dot{r}_v, \ddot{r}_e, \ddot{r}_n, \ddot{r}_v, a_e^{LF}, a_n^{LF}, \tau\}^T \quad (8)$$

where  $r_e$ ,  $r_n$  and  $r_v$  are the components of the baseline between the reference and rover antennas,  $\dot{r}_e$ ,  $\dot{r}_n$ ,  $\dot{r}_v$  are the velocity components of the rover,  $\ddot{r}_e$ ,  $\ddot{r}_n$ ,  $\ddot{r}_v$  are the corresponding acceleration components,  $a_e^{LF}, a_n^{LF}$  are the low frequency components of the rover acceleration not captured by the accelerometers, and  $\tau$  is the difference between the local clocks in the two GPS receivers.

We use a matrix  $\Phi$  to describe the relationship between the current state  $k$  and the next state  $k+1$  of the output quantity,  $x$ .

$$x_{k+1} = \Phi x_k + w_k \quad (9)$$

where  $w_k$  is process noise. Hence, the covariance matrix of the process noise  $w_k$  is

$$Q = E[w_k w_k^T] \quad (10)$$

Using the state transition matrix  $\Phi$ , we predict the next discrete state  $k+1$  of the position  $I = \{r_e, r_n, r_v\}$  as a linear function of the previous position, velocity and acceleration:

$$\bar{\Gamma}_{k+1} = \bar{\Gamma}_k + \Delta t \bar{v}_k + \frac{\Delta t^2}{2} \bar{a}_k \quad (11)$$

We model the acceleration and the clock difference as random walk processes. The low frequency parts of the accelerations are modeled as Gauss Markov processes.

*Random walk:*

We define a discrete random walk process,  $\mu$ , as a sampled Wiener process [8]

$$\mu_{k+1} = \mu_k + n_k \quad (12)$$

where  $n$  is a zero mean white noise sequence. Hence the best prediction of a random walk process value is the previous value of the process and thus the representing element in  $\Phi$  is equal to 1. The process noise covariance matrix can be written as

$$Q = \alpha \cdot \Delta t \quad (13)$$

where  $\alpha$  is a constant characterizing the process and  $\Delta t$  is the time between the samples  $k$  and  $k+1$ .

In order to find representative values for our acceleration parameter  $\alpha$ , we estimate  $Q$  for different  $\Delta t$ .

$$\hat{Q}(k) = \frac{1}{N} \sum (a_m(i) - a_m(i+k))^2 \quad (14)$$

where  $a_m$  is measured acceleration. Fig. 1 shows  $Q$  for a 27 s long data section. The green curve is based on measurements from the accelerometer mounted in the driving direction of the car and the red curve is based on a preliminary GPS acceleration estimates.

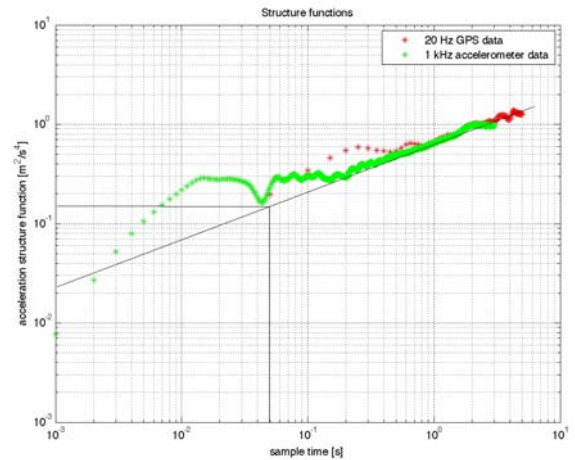


Fig. 1 Example of an estimate of  $Q$  based on measurements from the accelerometer (green) and GPS (red).

A fit to the data in the figure gives a value for  $\alpha$  that we use in our processing.

*Gauss Markov:*

We model the low frequency variations, not captured by the accelerometers, as a Gauss Markov processes which is a stationary Gaussian random process with an exponential autocorrelation function. The modeling is performed by describing the true acceleration,  $\ddot{r}$ , as the measured acceleration plus a slowly varying Gauss Markov process  $a_{GM}$ :

$$\ddot{r} = a_m + a_{GM} \quad (15)$$

The state of the Gauss Markov acceleration is in the Kalman filter modelled as.

$$a_{GM,k+1} = e^{-B\Delta t} a_{GM,k} + n \quad (16)$$

where  $e^{-B\Delta t}$  which describes the exponentially decaying correlation of the Gauss Markov, is the state transition factor used in the  $\Phi$  matrix to describe the Gauss Markov process and  $n$  is the process noise of the Gauss Markov process.

In order to characterize this Gauss Markov process, the accelerometer measurements are compared to GPS-only estimates of the acceleration. The difference between these two sets of measurements represents the low frequency process,  $a_{GM}$  that the accelerometers do not produce. We estimate the time constant  $1/B$  of the Gauss Markov process by analyzing the autocorrelation of this difference.

## MEASUREMENT UNCERTAINTY

We evaluate the measurement uncertainties using the Kalman filter error covariance matrix  $P$ . The diagonal elements of the matrix  $P$  contain the standard measurement uncertainties squared for each output quantity.  $P$  is determined for each epoch  $k$  as

$$P_k = (I - K_k H_k) P_k^- \quad (17)$$

where  $H$  is the observation matrix from the measurement model in (7),  $K$  is the Kalman gain, see [8], and  $P^-$  is the *a priori* error covariance. The *a priori* error covariance is a function of the state transition matrix  $\Phi$ , process noise covariance matrix  $Q$  and error covariance matrix  $P$  from the previous epoch,  $k-1$ .

$$P_k^- = \Phi_{k-1} P_{k-1} \Phi_{k-1}^T + Q_{k-1} \quad (18)$$

The process noise parameters, in the noise covariance matrix  $Q$ , are as described in the stochastic modelling statistically determined by structure functions from the driving dynamics of the car.

As described above the estimated state variables and the corresponding uncertainty in the Kalman filter is dependent on the models and parameters used in the Kalman filter. The measurement uncertainty used as input to the Kalman filter just propagates through the filter, hence good traceability is achieved. With proper modelling and accurately estimated noise parameters good control of the uncertainty estimates is possible.

## 5. RESULTS

We evaluated the system by an open-sky field experiment with the measurement system mounted in a car at a test location with minimal obstruction of the GPS signal. The experiment was performed 13.00-14.00 UTC on November 17, 2008. Measurements were collected during 15 minutes. The driving dynamics varied with velocities between 0 and 100 km/h and with both rapid accelerations and decelerations. Fig. 2 shows the speed estimate during an 85 second long section of the experiment. The initial part shows the speed of the car while driving at a freeway, the rapid decrease in speed at the end of the period corresponds to a rapid deceleration at a freeway exit.

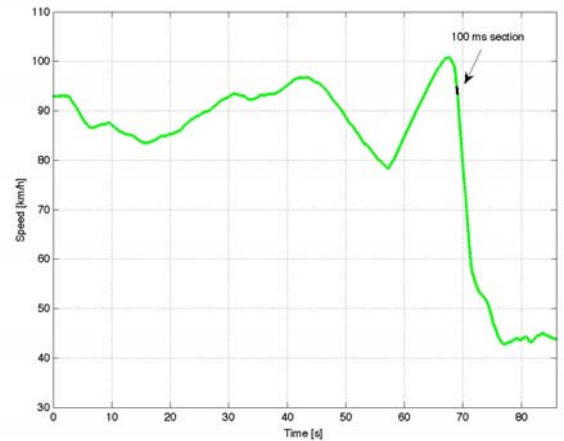


Fig. 2 Speed estimate during a period of 85 s (green). A 100 ms long section (black) of this period is presented in Fig.2.

Fig. 3 shows a 100 ms long section of the speed estimate. The section is a short snapshot during the deceleration shown in Fig. 2. In the figure is also shown the measurement uncertainties associated with each speed estimate. As can be seen, the expanded uncertainty is about  $\pm 0.2$  km/h using a coverage factor  $k=2$ . A slight increase in the measurement uncertainty can be seen during the periods with only accelerometer data.

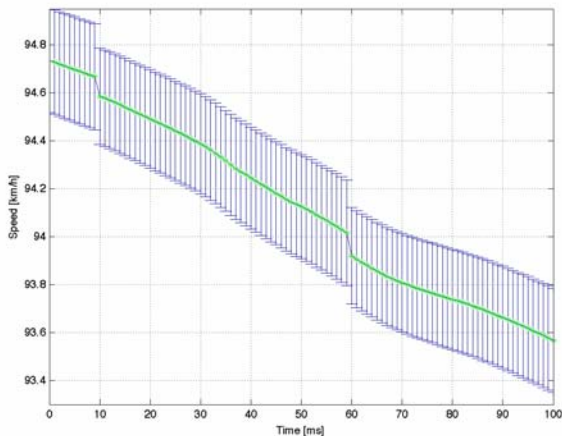


Fig. 3 Speed estimate during a 100 ms long period. The error bars in blue show the expanded measurement uncertainty with a coverage factor  $k=2$ .

## 6. DISCUSSION

The process noise parameters estimated in this experiment were estimated based on a 27 second long section of data from the 15 minute long experiment. The driving conditions during the experiment were as described varied with periods of very calm driving mixed with periods of driving with high dynamics. As a consequence, the process noise parameters may have been overestimated for applications with only low driving dynamics and slightly underestimated for very dynamical conditions. To improve the accuracy we could, for example, use process noise parameters that are determined from an independent data set with driving dynamics representative for the driving conditions of the specific application. For example the driving dynamics for a crash test application should be estimated from data collected from previous crash tests.

## 7. CONCLUSIONS

We have developed a system and methodology that provides position, velocity and acceleration estimates of high accuracy in the horizontal components with a time resolution of 1000 Hz. The method provides good control over the measurement uncertainties through the Kalman filter algorithm. However, independent evaluation should be performed in order to assess the results.

For future experiments we will extend the number of sensors e.g., use combined tri-axial accelerometers and gyros. By doing this all three acceleration components can be measured to improve the result, and the gyro information could be used for determining the direction of the car. To

utilize the gyro information the Kalman filter must be augmented with state variables corresponding to the gyro information. Furthermore to avoid the Gauss Markov modelling and to minimize the number of parameters that have to be estimated in the Kalman filter it is of interest to find accelerometers that provides DC information. Though when using accelerometers that provides DC information a study of how the gravity filed effects the result must be carried out to be able to compensate for this.

## REFERENCES

- [1] Smyth A., M. Wu, *Multi-rate Kalman filtering for the data fusion of displacement and acceleration response measurements in dynamic system monitoring*, Mechanical systems and Signal Processing , 2007, vol. 21
- [2] Wendel J., G. F. Trommer, *Tightly coupled GPS/INS integration for missile applications*, Aerospace Science and Technology, 2004, vol. 8
- [3] Gao J., M. G. Petovello and M. E. Cannon, Development of Precise GPS/INS/Wheel Speed Sensor/Yaw Rate Sensor Integrated Vehicular Positioning System, ION NTM, Monterey CA, 18-20 January 2006
- [4] Gao J., *GPS/INS/G Sensors/Yaw Rate Sensors/Wheel Speed Sensors Integrated Vehicular Positioning System*, ION GNSS, Forth Worth TX, 26-29 September 2006
- [5] Kim J., G. Jee, J. G. Lee, *A Complete GPS/INS Integration Technique Using GPS Carrier Phase Measurements*, Position Location and Navigation Symposium, IEEE 1998 Volume , Issue , 20-23 Apr 1998 Page(s):526 – 533, DOI: 10.1109/PLANS.1998.670208
- [6] Petovello, M.G., C. O'Driscoll and G. Lachapelle (2007) *Ultra-Tight GPS/INS for Carrier Phase Positioning in Weak Signal Environment*. NATO RTO SET-104 Symposium on Military Capabilities Enabled by Advances in Navigation Sensors, Antalya, Turkey, 1-2 October 2007, 18 pages.
- [7] Hoffmann-Wellenhof B., H. Lichtenegger and J. Collins, *GPS Theory and Practice*, Springer, New York, 1992.
- [8] Brown R. G., P. Y. C. Hwang, *Introduction to Random Signals and Applied Kalman Filtering*, Wiley, New York, 1992.